

$$g(\epsilon) = \frac{2\sqrt{2}}{\pi^2} K\left(\frac{1}{\sqrt{2}}\right) \frac{1}{\sqrt{\omega_2}} - \frac{\pi}{\sqrt{2}} \frac{\sqrt{|\Delta|}}{\omega_2 \omega_3}, \quad |\Delta| \ll \frac{\omega_3^4}{4}, \quad \Delta = \epsilon - \epsilon_2; \quad (6.10)$$

in a wider range, we find that

$$g(\epsilon) = \frac{2\sqrt{2}}{\pi^2} K\left(\frac{1}{\sqrt{2}}\right) \frac{1}{\sqrt{\omega_2}} \left[ 1 - \frac{|\Delta|^{1/4}}{\sqrt{2}\omega_2} \left( 2E\left(\frac{1}{\sqrt{2}}\right) - K\left(\frac{1}{\sqrt{2}}\right) \right) \right], \quad (6.11)$$

$$\frac{\omega_3^4}{4} \ll |\Delta| \ll \omega_2^2.$$

Throughout the frequency range, with the exception of narrow ( $\sim \omega_2^2$ ) intervals near the limits and near the middle of the spectrum the function  $g(\epsilon)$  is identical, apart from small corrections of the order of  $\omega_2^2$ , with the density of flexural vibrations of the corresponding planar lattice. Near the upper limit of the spectrum the behavior of  $g(\epsilon)$  is analogous to that of quasilongitudinal vibrations. Figure 5 shows schematically the behavior of  $g(\epsilon)$  for a quasiflexural branch.

The properties of local vibrations in a quasiflexural branch are also similar to the properties of vibrations polarized in the plane of a layer. It should be noted that if the difference between the behavior of the densities of vibrations in the limit  $\epsilon \rightarrow 0$  described by Eqs. (5.1a) and (6.2) had occurred in the optical zone, the conditions for the appearance (below the bottom of the zone) of local flexural vibrations near a heavy impurity would have been quite different from the case of vibrations polarized in the plane of a layer. The difference between the threshold values, due to the different behavior of the vibration density, would have ensured the existence of only local flexural vibrations for a wide range of impurity masses.

It must be stressed that the numbers and positions of the critical points of strongly anisotropic crystals have been obtained above for the simplest most symmetric case. In other situations the number of the critical points may be greater.

We shall conclude by pointing out that all the results obtained above apply equally well to the spectra of other excitations in strongly anisotropic crystals provided their dispersion law agrees with one of the types discussed above.

The author is grateful to I.M. Lifshitz, É.A. Kaner, and A.M. Kosevich for their interest in the above analysis and valuable discussions of the topics considered.

- <sup>1</sup>I. M. Lifshitz, Zh. Eksp. Teor. Fiz. 22, 475 (1952).
- <sup>2</sup>A. M. Kosevich, Osnovy mekhaniki kristallicheskoj reshetki (Fundamentals of Crystal Lattice Mechanics), Nauka, M., 1972.
- <sup>3</sup>I. M. Lifshitz, Zh. Eksp. Teor. Fiz. 17, 1017, 1076 (1947).
- <sup>4</sup>I. M. Lifshitz, Adv. Phys. 13, 483 (1964).
- <sup>5</sup>I. M. Lifshitz and A. M. Kosevich, Rep. Prog. Phys. 29, 217 (1966).
- <sup>6</sup>L. D. Landau and E. M. Lifshitz, Kvantovaya mekhanika, Nauka, M., 1974 (Quantum Mechanics: Non-Relativistic Theory, 3rd ed., Pergamon Press, Oxford, 1977).
- <sup>7</sup>L. D. Landau and E. M. Lifshitz, Statisticheskaya fizika, Nauka, M., 1976 (Statistical Physics, 3rd ed., Pergamon Press, Oxford, 1978), Part 1.
- <sup>8</sup>L. D. Landau and E. M. Lifshitz, Teoriya uprugosti, Nauka, M., 1965 (Theory of Elasticity, 2nd ed., Pergamon Press, Oxford, 1970).
- <sup>9</sup>Yu. Kagan and Ya. A. Iosilevskii, Zh. Eksp. Teor. Fiz. 42, 259 (1962); 44, 1375 (1963) [Sov. Phys. JETP 15, 182 (1962); 17, 926 (1963)].

Translated by A. Tybulewicz

## Quantum oscillations of the magnetoresistance of thin antimony ribbons

Yu. P. Gaïdukov and E. M. Golyamina

Moscow State University

(Submitted 13 January 1978)

Zh. Eksp. Teor. Fiz. 74, 1936-1949 (May 1978)

An investigation was made of the dependence of the derivative of the magnetoresistance of antimony whiskers on magnetic fields of 0-80 kOe intensity applied at temperatures of 1.3-4.2°K. These whiskers were broken up into ribbon-shaped samples with the following dimensions: thickness from 0.08 to 0.44  $\mu$ , width from 1.1 to 31  $\mu$ , and length from 0.2 to 3 mm. The size cutoff of quantum oscillations of the magnetoresistance was observed and investigated. It was also found that quantum oscillations appeared in truncated extremal electron orbits in fields below the cutoff value. These phenomena were predicted by A. M. Kosevich and I. M. Lifshitz in 1955 [Sov. Phys. JETP 2, 646 (1956)]. The experimental results indicated that the probability of specular reflection of conduction electrons from the surface of a sample was close to unity.

PACS numbers: 72.20.My, 72.20.Dp, 72.80.Cw

### INTRODUCTION

One of the important current problems in the physics of metals is the interaction of conduction electrons with the surface of a sample. The most interesting is

the case of specular reflection of electrons from the surface. The possibility of specular reflection has been demonstrated experimentally.<sup>1,2]</sup>

The interaction of electrons with a specularly reflec-

ting surface subject to the condition  $2r > d$  ( $r = cp_F/eH$  is the Larmor radius of the electron trajectory and  $d$  is the thickness of the sample) modifies the Landau level system and gives rise to new effects that are not found in bulk samples or in samples with diffusely scattering surfaces.

Quasiclassical quantization of the electron motion under conditions of specular reflection from the surface was first considered theoretically by Kosevich and Lifshitz in 1955.<sup>[3]</sup> Their calculation was carried out for oscillations of the magnetic moment of electrons but it applies also to the magnetoresistance oscillations, because the same authors showed later<sup>[4]</sup> that in strong fields characterized by  $r \ll l$  the oscillating part of the magnetoresistance of a compensated metal with convex Fermi surfaces obeys

$$\rho_{osc} \propto H^2 M_{osc} \quad (1)$$

( $l$  is the mean free path of electrons in a metal).

For the case of quantum oscillations in thin conductor plates the theory of Kosevich and Lifshitz<sup>[3]</sup> predicts a dependence of the oscillation period and amplitude on the applied magnetic field, thickness of the sample, and shape of the extremal sections of the Fermi surface in the range of magnetic fields in which the electron orbit diameter exceeds the thickness of the sample. This effect has not been observed experimentally until the investigation reported below. The main difficulty in studies of this kind has been the preparation of sufficiently thin high-quality samples with specularly reflecting surfaces.

We carried out an experimental study of quantum oscillations of the magnetoresistance of thin antimony ribbons and discovered the effect mentioned above. A preliminary communication of the results obtained was published earlier.<sup>[5]</sup>

## 2. SAMPLES AND MEASUREMENT METHOD

Our samples were made from whisker crystals. It is well known that whiskers are characterized not only by small dimensions but an extremely high quality of the structure in the bulk and on the surface, and also by a high chemical purity. Antimony is the most suitable material for the following reasons:

- The Fermi electron momentum in semimetals is low so that the probability of specular reflection from the surface is high;
- the Fermi surface of antimony is relatively simple and well known;
- attempts to grow samples have revealed that, unlike bismuth, crystals of antimony grow in the form of sufficiently thin and wide ribbons which are most convenient for measurements.

Such antimony whisker ribbons were grown for the first time by the present authors from the vapor phase.<sup>[6]</sup> The purity of the starting material was characterized by the resistivity ratio  $\rho_{293}/\rho_{4,2} \sim 1500$  (for a sample 1 mm thick). These whiskers were then separ-

TABLE I.

Sample No.	$d, \mu$	$\Delta, \mu$	$H_d, \text{kOe}$	$H_1, \text{kOe}$	$H_2, \text{kOe}$	$H_2/H_1$	$\Delta n_{\text{exp}}$	$n_d/4$	Type of carrier
Transverse field $H \parallel c_1 \perp I$									
29	0.08	7.0	—	50	—	—	—	—	—
44	0.10	5.3	45	28	36	1.3	3	4	—
43	0.13	11.1	43	27	34.2	1.3	3	4	$h_{\perp}$
48	0.13	5.3	38	23.8	30	1.3	3	4	$h_{\perp}$
41	0.14	6.4	38	26.8	31.7	1.2	3	4	$e_{\perp}$
34	0.14	7.5	38-50	27	32.4	1.2	3	4	—
69	0.21	30	29	17.5	22.8	1.3	5	6	$h_{\perp}$
72	0.22	10.9	26	15.9	20.6	1.3	4-5	6	$e_{\perp}, h_{\perp}$
35	0.22	16.8	26	14.6	19.1	1.3	4-5	7	$h_{\perp}$
58	0.24	1.1	21	7.4	13.7	1.8	4-5	8	$h_{\perp}$
73	0.25	1.3	30	6.4	11	1.7	4	8	$e_{\perp}$
45	0.42	5.1	14	5.2	9.2	1.8	8	12	$e_{\perp}$
62	0.43	12.0	15	7.7	10.2	1.3	7-8	12	$e_{\perp}, h_{\perp}$
63	0.44	31.0	—	4.7	7.7	1.6	8-9	12	$e_{\perp}$
Longitudinal field $H \parallel c_2 \parallel I$									
43	0.13	11.1	40-59	31	39	1.25	2	4	$h_{\parallel}$
69	0.21	30	32	19	25.5	1.3	4	6	$e_{\parallel}$

Note. The values of the fields  $H_d$ ,  $H_1$ , and  $H_2$  were found experimentally; the values of  $n_d$  were calculated. The type of carrier was determined from the SdH oscillation periods.

ated into ribbons with the following dimensions: thickness  $d = 0.08-0.44 \mu$ , width  $\Delta = 1.1-31 \mu$  (Table I), and length from 0.2 to 3 mm. All these ribbons were oriented in the basal plane of the crystal and the growth took place along the binary axis (Fig. 1a). The orientation of the samples was determined by measuring the anisotropy of the Shubnikov-de Haas (SdH) oscillation period and comparing the results obtained with those reported earlier;<sup>[7,8]</sup> information was also deduced from the direction of cleavage in the basal plane. The quality of the antimony whisker crystals used was characterized by the Dingle temperature  $T_D = 0.8 \pm 0.5^\circ \text{K}$  (electron orbit,  $H \parallel c_1$ ) and was high compared with the quality of bulk crystals of the same material, characterized by  $T_D = 3.4 \pm 1^\circ \text{K}$ .

A mounting method avoiding damage to the surface of the sample was developed: a whisker was placed on a plate made of Getinaks (plastic insulator) foil of  $7 \times 20$  mm dimensions with contact strips made of the foil and coated with an indium film (Fig. 1b). Contact was established because the smooth surface of the whisker adhered to indium; the assembly was reinforced by bonding the ends of the whisker with an adhesive containing a conducting filler. Four of the shorter whiskers (out of fifteen investigated) were mounted in such a way that they had two contacts (Fig. 1c). The distance between the potential contact strips was  $L = 100-700 \mu$ ; it was measured under a MIM-7 microscope to within  $\pm 5 \mu$ . After completion of all the measurements, the whisker was removed from the contacts

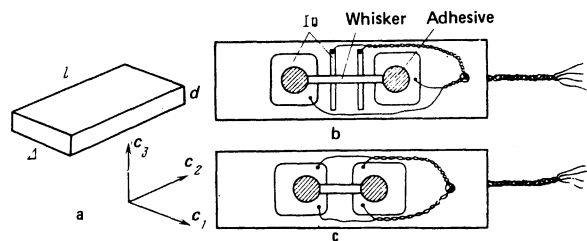


FIG. 1. a) Schematic representation of ribbon-shaped antimony whisker. b, c) Sample mounted on a base with four and two contacts.

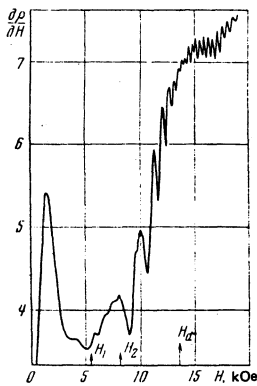


FIG. 2. Derivative of the magnetoresistance of sample Sb-45,  $d=0.42 \mu$ , recorded at  $T=1.4^\circ\text{K}$ . Here, and in Figs. 3-5, the arrows identify the calculated cutoff fields and the first two peaks; the derivative is shown on an arbitrary scale.

and placed on a quartz substrate where its thickness was determined by the interference method.<sup>[9]</sup> This thickness was found to within 10%. The thickness measurements were accompanied by determination of the whisker width to within  $\pm 0.15 \mu$ .

At room temperature the resistivity determined from the total resistance and geometry was found to be within the range  $(40-50) \times 10^{-6} \Omega \cdot \text{cm}$  and at helium temperatures it was  $(0.5-1.5) \times 10^{-6} \Omega \cdot \text{cm}$ ; so significant dependence on the thickness was found.

The galvanomagnetic measurements were carried out at temperatures of 1.3-4.2°K in magnetic fields of 0-80 kOe. The oscillatory effects were recorded by a modulation method of measuring the magnetoresistance derivative  $\partial\rho(H)/\partial H$ .

### 3. RESULTS OF MEASUREMENTS

Figures 2-5 give examples of records of the derivative of the magnetoresistance of samples of different thickness. The SdH oscillations, observed in strong fields, vanished at  $H_d$  and in weaker fields  $H < H_d$  there appeared a group of new oscillation peaks of the derivative  $\partial\rho(H)/\partial H$ . We shall show in a discussion of the results that the field  $H_d$  was the "cutoff field" at which the condition  $2r=d$  was satisfied.

We shall now consider in greater detail the experimental curves in Figs. 2-5.

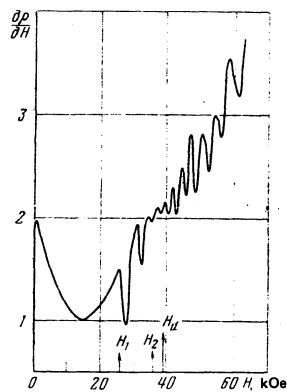


FIG. 3. Derivative of the magnetoresistance of sample Sb-41,  $d=0.14 \mu$  thick, recorded at  $T=4.2^\circ\text{K}$ .

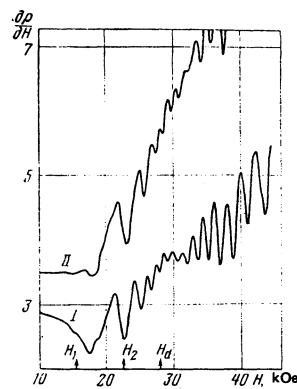


FIG. 4. Dependences of the derivative of the magnetoresistance on the transverse magnetic field applied to sample Sb-69,  $d=0.21 \mu$  thick, at  $T=1.4^\circ\text{K}$ : I) field  $H$  in the plane of the sample,  $H \parallel c_1$ ; II) field  $H$  inclined to the plane of the sample at  $\theta=18^\circ$ .

3.1. In a magnetic field perpendicular to the electric current and parallel to the plane of the ribbon, i.e., in  $H \parallel c_1$ , the SdH oscillation periods in fields  $H > H_d$  corresponded to small sections of the electron and hole Fermi surfaces of antimony with periods in the interval  $\Delta(H^{-1}) \sim (13-15) \times 10^{-7} \text{Oe}^{-1}$  (Figs. 2 and 3 and curve I in Fig. 4). The new peaks observed in weak fields  $H < H_d$  were of completely different nature and were characterized by the following features: a) the separation between these peaks as well as their amplitude increased on reduction of  $H$ ; b) the number of the peaks  $\Delta n$  was limited and much smaller than the total number of the SdH peaks in fields  $H_d < H < \infty$ ; c) an increase in the thickness of the sample did not alter basically the effect but the range of existence of the new peaks shifted toward weaker fields and their number increased; d) the field  $H_1$  corresponding to the first peak on the weak-field was comparable with the field  $H_d$  ( $0.3H_d < H < H_d$ ) and reached values of 20-30 kOe for the thinnest samples.

3.2. Rotation of a ribbon in a magnetic field about the  $c_2$  axis,<sup>1)</sup> resulting in an increase of the angle  $\theta = \angle(H, c_1)$ , shifted the new peaks somewhat toward higher fields, reduced their amplitude, and caused the monotonic part of the derivative to rise deeply (curve II in Fig. 4). The peaks practically disappeared when the angle of inclination of the field to the plane of the ribbon reached  $\theta \sim 30^\circ$ . In a field perpendicular to the plane of the ribbon,  $H \parallel c_3$ , the oscillations were of the conventional SdH type with a period of  $\Delta(H^{-1}) \approx 10 \times 10^{-7} \text{Oe}^{-1}$  right down to weak fields of  $\sim 7$  kOe in which the oscillation amplitude became comparable with the noise

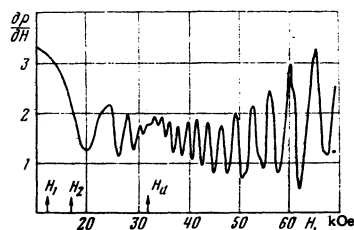


FIG. 5. Dependence of the derivative of the magnetoresistance on the magnetic field parallel to the current applied to sample Sb-69,  $d=0.21 \mu$  thick, at  $T=1.4^\circ\text{K}$ .

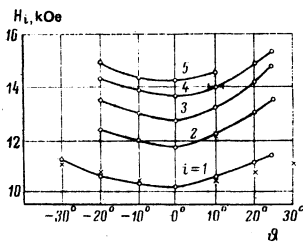


FIG. 6. Shift of the positions of the peaks in  $H < H_d$  as a function of the angle of inclination  $\theta$  of the field  $H$  relative to the plane of sample Sb-62,  $d = 0.43 \mu$  thick:  $\circ$ ) experimental positions of the fields  $H$  corresponding to peaks;  $\times$ ) calculated positions of the first peak.

background.

The displacement of the new peaks on inclination of the field relative to the ribbon plane is shown in Fig. 6 for sample Sb-62.

3.3. In the longitudinal orientation of the field,  $H \parallel c_2 \parallel I$ , new peaks were again observed (Fig. 5) and the field  $H_d$  was approximately the same as for  $H \parallel c_1$ , whereas the peak positions differed somewhat.

3.4. We shall now consider for which sections of the Fermi surface the cutoff of the SdH oscillations should take place, i.e., which groups of carriers should dominate the contribution to the oscillating part of the conductivity in fields  $H > H_d$ .

For all the samples with the exception of two (Sb-58 and Sb-73) the SdH periods in the field  $H \parallel c_1 \perp I$  corresponded to small cross sections of the hole and electron Fermi surfaces:  $\Delta(H^{-1})_h = 13.3 \times 10^{-7} \text{Oe}^{-1}$  and  $\Delta(H^{-1})_e = 14.9 \times 10^{-7} \text{Oe}^{-1}$  (Ref. 7). We shall denote the corresponding "ellipsoids" of the Fermi surface of antimony by  $h_I$  and  $e_I$ . The other "ellipsoids" with larger cross sections for the same direction of the field  $H$  will be denoted by  $h_{II}$  and  $e_{II}$ . Oscillations due to these extremal sections were observed in samples Sb-58 and Sb-73 and the periods were within the range  $\Delta(H^{-1}) \sim (7-8) \times 10^{-7} \text{Oe}^{-1}$ .

Table I lists, in accordance with this notation, the groups of carriers dominating the oscillatory part of the magnetoresistance in fields  $H > H_d$ , the experimental values of the fields  $H_d$ , the fields corresponding to the first two peaks  $H_1$  and  $H_2$ , and the number of peaks  $\Delta n$  in the range  $0-H_d$ .

## 4. DISCUSSION OF RESULTS

### 4.1. $H \geq H_d$ . Cutoff of quantum oscillations

The interpretation of the field  $H_d$  as the field in which the SdH oscillations are cut off by the size of the sample is proved in Fig. 7. This figure gives the experimental values of the field  $H_d$  as a function of  $d^{-1}$  and two straight lines corresponding to the theoretical dependence of the cutoff field in the  $2r = d$  case:  $H_d = 2p_2c/ed$ , where  $p_2$  is the quasimomentum along the  $c_2$  axis, which governs (in the field  $H \parallel c_1$ ) the size of the electron orbit at right-angles to the current  $I \parallel c_2$ . One line is drawn for the  $h_I$  holes ( $p_2 = 4.6 \times 10^{-21} \text{g}\cdot\text{cm}\cdot\text{sec}^{-1}$ ) and the other for the  $e_I$  electrons ( $p_2 = 5.3 \times 10^{-21} \text{g}\cdot\text{cm}\cdot\text{sec}^{-1}$ ).

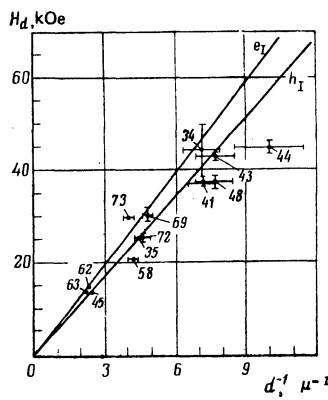


FIG. 7. Experimental values of the cutoff field  $H_d$  for samples of different thickness (Table I) obtained for  $H \parallel c_1$ . The lines represent the dependences  $H_d = 3p_2c/ed$  for the  $h_I$  holes ( $p_2 = 4.6 \times 10^{-21} \text{g}\cdot\text{cm}\cdot\text{sec}^{-1}$ ) and  $e_I$  electrons ( $p_2 = 5.3 \times 10^{-21} \text{g}\cdot\text{cm}\cdot\text{sec}^{-1}$ ).

Here and later, we shall use the quasimomenta taken from Ref. 10. The large number of points fits, within the limits of the experimental error, the line for  $h_I$  but the two lines are close to one another. We do indeed find that for the majority of the thin samples subjected to strong fields  $H > H_d$  the main SdH oscillation period corresponds to the  $h_I$  hole group and only thicker samples, with  $d > 0.4 \mu$ , show more clearly the influence of the  $e_I$  electron group (Table I).

In a longitudinal field the value of  $H_d$  is the same one as in the transverse field. This can be explained by the fact that in  $H \parallel c_2$  this field is given by  $H_d = 2p_1c/ed$ , where  $p_1 = 6.3 \times 10^{-21} \text{g}\cdot\text{cm}\cdot\text{sec}^{-1}$  for the  $h_{II}$  holes or  $p_1 = 5.3 \times 10^{-21} \text{g}\cdot\text{cm}\cdot\text{sec}^{-1}$  for the  $e_{II}$  electrons, i.e., the momenta  $p_1$  are close to  $p_2$  for  $h_I$  and  $e_I$  governing the field  $H_d$  in the  $H \parallel c_1$  case.

### 4.2. $H < H_d$ . Quantum oscillations for truncated orbits

We shall consider the nature of the new effect observed in fields below the cutoff value and we shall show that it is associated with the quantization of the electron motion in an extremal orbit which is truncated by the two surfaces of the sample. In fields  $H < H_d$  for  $n \gg 1$  ( $n$  is the number of the Landau levels) the theory of Kosevich and Lifshitz<sup>[3]</sup> predicts a strong dependence of the oscillation period on the shape of the extremal section as well as on the magnetic field and plate thickness  $d$ . The experimental results can be used to draw conclusions on the period and its changes only when the number of the observed peaks is large. However, in our case the number of new resistance peaks is  $\Delta n \sim 3-7$ . The direct application of the general theoretical expressions<sup>[3]</sup> to the experimental results would have been too cumbersome and inconvenient. A qualitative analysis of the effect, which will be given below, is based on simple physical ideas about the quantization of the electron motion in a magnetic field and it allows us to establish a number of relationships and to estimate the positions of the magnetoresistance singularities along the magnetic field scale when the number of these singularities is small.

Figure 8a shows the dependence of the number of

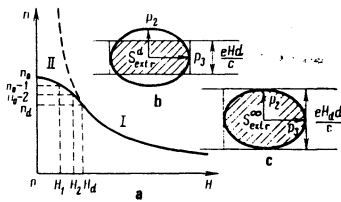


FIG. 8. a) Dependence of the number of quantum levels on the magnetic field: I)  $H > H_d$ , conventional SdH effect; II)  $H < H_d$ , oscillations for extremal orbits truncated by two surfaces of a ribbon-shaped sample. b) Extremal section through the Fermi surface truncated by two surfaces of a thin ribbon of thickness  $d$ . c) Extremal section in a field equal to the cutoff value  $H = H_d$ .

filled quantum levels  $n$  on the magnetic field  $H$ . In fields  $H > H_d$  we have the conventional SdH effect and  $n$  is found from

$$S_{\text{extr}}^{\infty} = \frac{2\pi\hbar e H}{c} \left( n + \frac{1}{2} \right), \quad (2)$$

from which it follows that  $n \propto H^{-1}$ . Here,  $S_{\text{extr}}^{\infty}$  is the area of an untruncated extremal electron orbit in the momentum space.

In fields  $H < H_d$  an extremal electron orbit no longer fits inside the sample and the electron motion changes significantly. Figure 8b shows, in the momentum space, an elliptic section of the Fermi surface with semi-axes  $p_3$  and  $p_2$  in a magnetic field  $\mathbf{H} \parallel c_1$  cut off by the size of the sample  $eHd/c$ . It corresponds to an extremal electron orbit in the momentum space on condition that electrons are reflected specularly from the surface of the sample. Moreover, the sections should satisfy the quantization condition

$$S_{\text{extr}}^d = \frac{2\pi\hbar e H}{c} \left( n + \frac{1}{2} \right) \quad (3)$$

(which shall ignore the correction  $\frac{1}{2}$ ). Using Eq. (3) and Fig. 8b, we can easily find the limit to which the number  $n$  tends for  $H \rightarrow 0$ :

$$n_0 = \lim_{H \rightarrow 0} n = \frac{c}{2\pi\hbar e H} \left( 2p_3 \frac{eHd}{c} \right) = \frac{p_3 d}{\pi\hbar}. \quad (4)$$

The number of filled levels in the field  $H_d$  is a function of the SdH oscillation period:

$$n_d = \frac{1}{H_d \Delta(H^{-1})} = \frac{S_{\text{extr}}^{\infty} d}{4\pi\hbar p_2}. \quad (5)$$

Thus, the number of the resistance singularities in fields  $0 < H < H_d$  is equal to  $\Delta n = |n_0 - n_d|$ . Using the extremal section area  $S_{\text{extr}}^{\infty} = \pi p_2 p_3$ , we obtain

$$\Delta n = n_0 - n_d = \frac{p_3 d}{\pi\hbar} - \frac{p_3 d}{4\hbar} \approx \frac{n_d}{4}. \quad (6)$$

Table I lists for every sample the value of  $n_d/4$  calculated from the experimental values of  $H_d$  and  $\Delta(H^{-1})$  as well as the number  $\Delta n_{\text{exp}}$ , equal to the number of new  $\partial\rho/\partial H$  peaks observed in fields  $H < H_d$ . We can see that  $\Delta n_{\text{exp}}$  is approximately 20–30% less than the corresponding value of  $n_d/4$ . This small disagreement may be attributed to the nonellipticity of the corres-

ponding section of the Fermi surface of antimony. (For example, if the section is a rectangle, there should be no peaks for  $H < H_d$  because  $\Delta n = 0$ .)

The positions  $H_i$  of the peaks in fields  $H < H_d$  are found from

$$n_0 - n(H_i) = i, \quad i = 1, 2, \dots, \Delta n. \quad (7)$$

This is an approximate expression because the crossing of the  $n$ -th Landau level by the Fermi level is associated with the position of the corresponding minimum of the curve  $\partial\rho/\partial H = f(H)$ . In fact, this crossing depends on the phase of the quantum oscillations, which is governed by the factor  $\gamma$  in the quantization law  $S_{\text{extr}} = 2\pi e\hbar c^{-1} H(n + \gamma)$ , shape of the electron trajectory, and spin splitting of the Landau levels.<sup>[11]</sup> For example, in the quasiclassical approximation and for a convex trajectory without points of inflection ( $\gamma \approx 1/2$ ) the point of crossing of the level is displaced by  $+\pi/4$  relative to the minimum of the oscillatory function

$$\frac{\partial\rho}{\partial H} \propto \sin\left(\frac{cS_{\text{extr}}}{e\hbar H} - \frac{\pi}{4} - \pi\right).$$

Thus, the above calculations of the peaks are approximate (to within half a distance between them) but the relative separations can be found exactly.

Application of Eqs. (3) and (4) gives

$$n_0 - n(H) = \frac{c}{2\pi\hbar e H} (S_r(H) - S_{\text{extr}}^d(H)) = \frac{c}{2\pi\hbar e H} \Delta S(H), \quad (8)$$

$$S_r(H) = 2p_3 e H d / c.$$

It should be noted that: a) the condition (8) is formally analogous to the condition of quantization for the area  $\Delta S(H) = S_r(H) - S_{\text{extr}}^d(H)$ ; b) it follows from Eq. (8) that  $\Delta n = (c/2\pi\hbar e H) \Delta S(H)$ —see Fig. 8c.

We shall estimate the values of  $H_1$  and  $H_2$  corresponding to the first two peaks on the weak-field side. In weak fields we may assume that the extremal section  $S_{\text{extr}}^d$  is limited by two parallel lines passing at a distance  $\pm eHd/2c$  from the center and by arcs of a circle of radius  $p_3$  (in fact, the cross sections of interest to us differ from a circle by  $\pm 10\%$ ). Then, to a term of the third order in  $H$ , the difference between the areas  $\Delta S$  can be written in the form

$$\Delta S \approx 4 \left( \frac{eHd}{2c} \right)^2 \frac{1}{6p_3}.$$

Using the condition (7) with  $i = 1$ , we find the field corresponding to the first peak:

$$H \approx \frac{5c}{e} \left( \frac{\pi\hbar p_3^3}{d^2} \right)^{1/2}. \quad (9)$$

Similarly, for  $i = 2$ , we obtain  $H_2 \approx H_1 \sqrt{2}$ .

We shall now compare these relationships with the experimental data. Figure 9 gives the experimental values of the field  $H_1$  corresponding to the first peak of samples of different thickness and lines based on Eq. (9) for the  $h_T$  hole ( $p_3 = 5.7 \times 10^{-21}$  g·cm·sec<sup>-1</sup>) and  $e_T$  electron ( $p_3 = 4.3 \times 10^{-21}$  g·cm·sec<sup>-1</sup>) Fermi surfaces. The deviations of the experimental points from the depend-

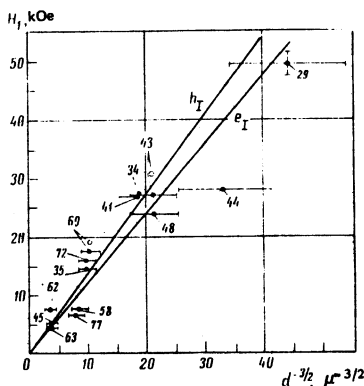


FIG. 9. Field of the first peak  $H_1$  for samples of different thickness  $d$ : ●)  $H \parallel c_1 \perp I$ ; ○)  $H \parallel c_2 \parallel I$ .

ence (9) may be attributed to the error in the determination of the thickness of the samples and to the departure of the shape of the section from the circle. Since the values of the field  $H_1 \propto \sqrt{p_3}$  for the  $h_I$  holes and  $e_I$  electrons differ by less than 15%, it is difficult to determine which of these two groups of carriers is responsible for the first peak of the dependence  $\partial\rho(H)/\partial H$ .

Table I lists also the values of the fields  $H_2$  corresponding to the second peaks and of the ratio  $H_2/H_1$  found experimentally. We can see that  $H_2 \approx H_1\sqrt{2}$  to within  $\pm 30\%$ . For thinner samples with  $d \leq 0.2\mu$ , characterized by pure hole SdH oscillations in fields  $H > H_d$ , the ratio is  $H_2/H_1 = 1.27 \pm 4\%$ , whereas for the two thicker samples with  $d > 0.4\mu$  with pure electron oscillations the ratio is  $H_2/H_1 = 1.7 \pm 4\%$ . These deviations of the ratio  $H_2/H_1$  from  $\sqrt{2}$  may be explained by the deviation of the shape of the Fermi sections from the circle, and also by the difference between the shapes of the hole and electron sections.

The lower values of the field  $H_1$  for samples Sb-58 and Sb-73, compared with other samples, can be explained in a natural manner by the smaller curvature of the  $h_{II}$  and  $e_{II}$  cutoff sections bearing in mind that their dimensions represented by  $p_3$  are approximately the same as those for  $e_I$  and  $h_I$ .

The large deviation of the point  $H_1$  for sample Sb-44 from the general dependence can be explained only by the fact that there may have been an error in the determination of the number of the interference fringes in the course of the measurement of its thickness.

The experimental values of  $H_1$ ,  $H_2$ , and  $H_d$  obtained in the longitudinal field  $H \parallel c_2 \parallel I$  are approximately the same as those obtained in the transverse field  $H \parallel c_1 \perp I$  because the dimensions of the cutoff sections are similar for both cases.

### 4.3. Determination of the shape of extremal sections of the Fermi surface from positions of $H_i$ peaks in fields $H < H_d$

We shall now demonstrate the possibility of solving the problem which is the inverse of that solved in Sec. 4.2.

Employing the expressions (7) and (8), we can find the area of the truncated extremal section  $S_{\text{extr}}^d(H_i)$ .

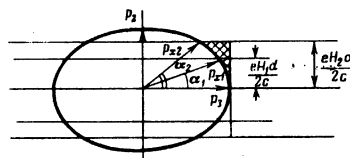


FIG. 10. Determination of the shape of a section of the Fermi surface based on the positions of the peaks  $H_i$  on the magnetic field scale;  $i=1, 2, \dots$

Knowing a set of values of such areas, we can reconstruct the exact shape of the section. A reliable calculation can be carried out for the electron section because the electron Fermi surface of antimony has the central symmetry and reflection symmetry relative to the trigonal-bisector plane.

The calculations are explained in Fig. 10 and they are based on Eqs. (7) and (8). The difference between the areas of a rectangle  $S_r(H)$  and a section  $S_{\text{extr}}^d$  can be represented by a sum of a right-angled triangle (for  $H_1$ ) and a trapezium shown shaded in Fig. 10:

$$4 \left\{ \frac{1}{2} \frac{eH_1 d}{2c} (p_3 - p_1 \cos \alpha_1) \right\} \frac{c}{2\pi \hbar e H_1} = 1, \quad \sin \alpha = \frac{eH_1 d}{2c p_{x,1}}$$

is the condition for the first peak,

$$4 \left\{ \frac{1}{2} (p_3 - p_{x,1} \cos \alpha_1 + p_3 - p_{x,2} \cos \alpha_2) \left( \frac{eH_2 d}{2c} - \frac{eH_1 d}{2c} \right) + \frac{1}{2} (p_3 - p_{x,1} \cos \alpha_1) \frac{eH_1 d}{2c} \right\} \frac{c}{2\pi \hbar e H_2} = 2, \quad \sin \alpha_2 = \frac{eH_2 d}{2c p_{x,2}}$$

is the condition for the second peak, and so on.

Such a calculation was carried out for two samples, Sb-63 and Sb-45, exhibiting electron SdH oscillations and it was used to reconstruct the shape of the small section of the electron Fermi surface (Fig. 11). The results indicate that the section differs little from the ellipse although it is slightly more convex. The plot in Fig. 11 is based on the values of  $p_3$  ( $\alpha = 0$ ) and  $p_2$  ( $\alpha = 90^\circ$ ) taken from Ref. 10. (Generally speaking, this procedure is not necessary if we know the exact values of  $H_d$  and  $\Delta n$ .)

The above expressions allow us to calculate for each

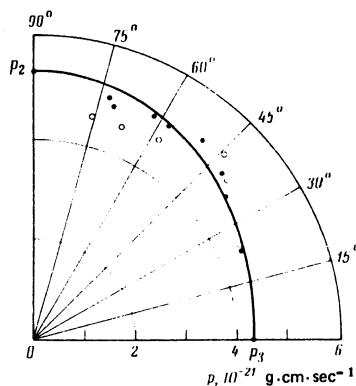


FIG. 11. Plotting of a section of the Fermi surface of antimony on the basis of the positions of the oscillation peaks  $H = H_i$  on the magnetic field scale: ●) sample Sb-63,  $d = 0.44 \mu$ ; ○) sample Sb-45,  $d = 0.42 \mu$ .

peak the angles at which electrons or holes are incident on the surface of a sample:  $\varphi_i = 90 - \alpha_i$ . For electrons these angles are within the range  $\varphi_i \sim 30^\circ - 70^\circ$  and they should be the same for holes.

Since the oscillations associated with the extremal truncated orbits may exist only in the case of specular reflection from the surface, we can say that the probability of such reflection in our samples is close to unity even for large angles of incidence of electrons and holes on the surface.

#### 4.4. Effect of inclination of a magnetic field relative to the plane of a sample

When the field  $H$  is inclined at an angle  $\vartheta$  moving from the  $c_1$  to the  $c_3$  axis, the extremal size  $p_2$  of the corresponding orbit in the momentum space is not affected and the other semiaxis of the orbit becomes

$$p_o = \left( \frac{\sin^2 \vartheta}{p_1^2} + \frac{\cos^2 \vartheta}{p_3^2} \right)^{-1/2}, \quad (10)$$

$$p_o|_{\vartheta=0} = 4.3 \cdot 10^{-21} \text{ g} \cdot \text{cm} \cdot \text{sec}^{-1}$$

$$p_o|_{\vartheta=90^\circ} = 20 \cdot 10^{-21} \text{ g} \cdot \text{cm} \cdot \text{sec}^{-1}$$

However, in real space the inclination of the plane of the  $e_1$  orbit is practically zero because for small angles  $\vartheta$  the Fermi surface differs little from a cylinder. Consequently, the cutoff field  $H_d$  should be independent of  $\vartheta$  and the position of the first peak should, according to Eq. (9), vary in accordance with the law

$$H_1 \propto p_o^{1/2} \propto (p_3 / \cos \vartheta)^{1/2}. \quad (11)$$

Figure 6 shows the measured dependence of  $H_1$  on the angle of inclination of the field as well as the values of  $H_1$  calculated from Eq. (11). The asymmetric positioning of the experimental points relative to the angle  $\vartheta = 0$  is clearly due to inclination by  $7-8^\circ$  of the major semiaxis of the electron "ellipsoid" of the Fermi surface relative to the  $c_1$  bisector axis.<sup>[7,10]</sup>

#### 4.5. Amplitude of $\partial\rho/\partial H$ oscillations in fields $H < H_d$

Since the Fermi surface sections  $e_1$  and  $h_1$  in  $H \| c_1$  differ by not more than  $\pm 10\%$  from the circle, we shall continue our analysis for the case of a circular section.

For the SdH oscillations in a bulk conductor the amplitude dependence is of the form<sup>[4,11,12]</sup>

$$A_H \propto H^{1/2} \exp \left\{ -2\pi^2 k(T+T_D) / \hbar \omega^* \right\}, \quad (12)$$

where  $\omega^* = eH/m^*c$  is the cyclotron frequency of electron revolution on a circular orbit in a field  $H$  and  $T_D$  is the Dingle temperature for the scattering in the bulk of a metal.

The revolution frequency is different for a thin conductor subjected to a field  $H < H_d$  and characterized by truncated orbits (Fig. 12a). Figure 12b shows a truncated electron trajectory in the coordinate space. The revolution frequency along this trajectory is

$$\omega^d(H) = \frac{\pi}{2} \frac{eH}{m^*c} \frac{1}{\arcsin(H/H_d)} = \omega^*(H) \frac{\pi}{2} \frac{1}{\arcsin(H/H_d)},$$

or, in terms of the reduced magnetic field  $x = H/H_d$ ,

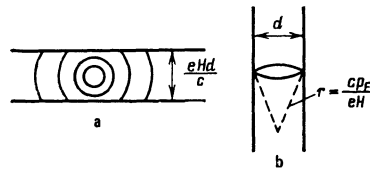


FIG. 12. a) System of Landau levels in the momentum space derived for a thin plate with a spherical Fermi surface, subjected to a field  $H$ . b) Truncated extremal orbit of an electron in a field  $H$  in the coordinate space.

$$\omega^d(x) = \frac{\pi}{2} \omega^*(H_d) \frac{x}{\arcsin x}. \quad (13)$$

This dependence is shown graphically in Fig. 13.

We can see that the simple exponential dependence of the field in Eq. (12) for fields  $H > H_d$  becomes much more complicated in fields  $H < H_d$  because of the nonlinear variation  $\omega^d(H)$ :

$$A_H^d \propto H^{1/2} \exp \left\{ -2\pi^2 \frac{k(T+T_D')}{\hbar \omega^d(H)} \right\},$$

where  $T_D'$  represents the electron scattering in the bulk and (mainly) on the surface of the sample, governed by the angle of incidence of electrons on the surface. Thus, a special size dependence of the oscillation amplitude on the field  $H$  and on the sample thickness  $d$  is observed.

The oscillation amplitude was calculated by a rigorous mathematical method in the paper by Kosevich and Lifshitz.<sup>[3]</sup> Using the fact that  $\partial\rho_{osc}/\partial H \propto HM_{osc}$ , we find that in the case of an electron gas with a quadratic isotropic dispersion law, the expression (14) in the paper by Kosevich and Lifshitz,<sup>[3]</sup> gives for  $x > 1$

$$A_x^d = (1-x^{-1}) A_x^* \propto (1-x^{-1}) x^{1/2} \exp \left\{ -\frac{2\pi^2 k(T+T_D)}{x \hbar \omega^*(H_d)} \right\}. \quad (14)$$

It follows from Eq. (12) of Kosevich and Lifshitz<sup>[3]</sup> that for  $x < 1$ ,

$$A_x^d \propto \frac{\arcsin x - [x^2(1-x^2)]^{1/2}}{(\arcsin x)^{1/2} [x^2/(1-x^2)]^{1/4}} \exp \left\{ -\frac{4\pi \arcsin x}{x} \frac{k(T+T_D')}{\hbar \omega^*(H_d)} \right\}. \quad (15)$$

It is clear from Eq. (14) that in strong fields  $x \gg 1$  the amplitude of oscillations in a thin sample behaves in the same way as in a bulk sample. Near the cutoff field in the limit  $x \rightarrow 1+0$  the oscillation amplitude vanishes exactly as in the limit  $x \rightarrow 1-0$  [see Eq. (15)].

Figure 14 shows a graph of the oscillations amplitude as a function of the magnetic field  $x = H/H_d$ , based on Eqs. (14) and (15). The Dingle temperature for fields

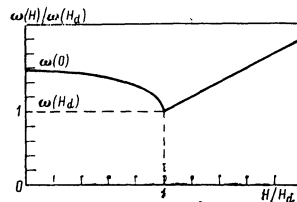


FIG. 13. Dependence of the cyclotron mass on the magnetic field. The axes give the values reduced to the cutoff field  $H_d$ .

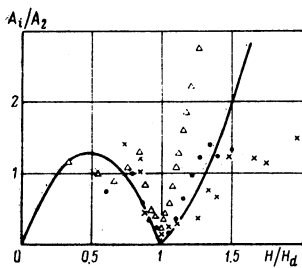


FIG. 14. Dependence of the amplitude of the oscillations of the derivative of the magnetoresistance reduced to the amplitude of the second peak  $A_2$  on the reduced magnetic field  $H/H_d$  with the  $\mathbf{H} \parallel c_1 \perp \mathbf{I}$  orientation:  $\times$ ) Sb-35,  $d=0.22 \mu$ ,  $T=1.5^\circ\text{K}$ ;  $\bullet$ ) Sb-69,  $d=0.21 \mu$ ,  $T=1.4^\circ\text{K}$ ;  $\Delta$ ) Sb-63,  $d=0.44 \mu$ ,  $T=1.4^\circ\text{K}$ . The continuous curve represents the amplitude of the quantum oscillations calculated on the basis of Eqs. (14) and (15).

$H < H_d$  is assumed to be  $T'_D = T_D = 1^\circ\text{K}$ . The field dependence of this amplitude is in full agreement with the experimental data given in the same figure: there is a characteristic fall of the amplitude to zero in the limit  $H \rightarrow H_D$  and an increase of this amplitude on both sides of this point.

We shall illustrate this point additionally by considering the positions of the quantum energy levels in a thin plate. The separation between these levels near the Fermi surface is governed by the cyclotron frequency:  $\Delta\epsilon = \hbar\omega$ . In fields  $H > H_d$  there are no truncated orbits and the levels are equidistant:  $\Delta\epsilon = \hbar\omega \propto H$ , the number of the filled levels in such fields being  $n = \epsilon_F / \Delta\epsilon \propto H^{-1}$ . In fields  $H < H_d$  the energy levels in the momentum space have the form shown in Fig. 12a. The distance between the lower untruncated levels should obey  $\Delta\epsilon \propto H$ , whereas the distance between the upper levels is, in accordance with Fig. 13,

$$\Delta\epsilon^d(H) = \hbar\omega^d(H) = \frac{\pi\hbar}{2} \omega^*(H_d) \frac{H/H_d}{(H/H_d)}$$

i.e.,  $\Delta\epsilon^d(H) > \Delta\epsilon^*(H)$  in fields  $H < H_d$ .

Thus, although the number of the filled levels increases by a finite amount  $\Delta n$  on reduction of the field from  $H_d$  to  $H=0$ , the distance between the upper levels increases. The positions of  $H$  are shown schematically in Fig. 15. The unusual distribution of the quantum levels in a magnetic field is responsible for the characteristic dependences of the period and amplitude of the quantum oscillations in thin samples on the field  $H$  and sample thickness  $d$ .

We note that in  $H=0$  there is a set of quantum energy levels of conduction electrons. Clearly, these levels simply represent the results of size quantization of the energy of electrons characterized by the quasimomentum  $p_3$  and moving in the coordinate space along the  $c_3$  axis between two surfaces of a plate of thickness  $d$ .

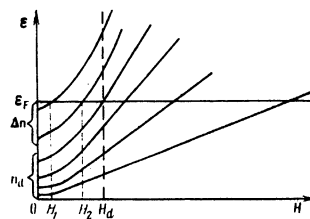


FIG. 15. Energy of the Landau levels in a thin plate plotted as a function of the magnetic field.

Our comparison of the experimental results with the theory thus confirms interpretation of the observed effect as the cutoff of the quantum oscillations of the magnetoresistance by the dimensions of a ribbon-shaped sample under conditions of almost specular reflection of electrons from the surfaces and as the appearance (in fields less than the cutoff value) of quantum oscillations of the magnetoresistance in extremal electron orbits cut off by the thickness of the sample, as predicted by Kosevich and Lifshitz.

The observed effect allows us, in principle, to determine the shape and dimensions of the extremal sections of the Fermi surface from the positions of the peaks in fields  $H < H_d$ , and also the characteristics of the surface scattering of the selected groups of carriers from the dependence of the amplitudes of these peaks on the field.

<sup>1</sup>The system of axes  $c_1$ ,  $c_2$ , and  $c_3$  will be taken as linked to the sample in the way shown in Fig. 1a.

<sup>2</sup>M. S. Khaikin, Usp. Fiz. Nauk 96, 409 (1968) [Sov. Phys. Usp. 11, 785 (1969)].

<sup>3</sup>V. S. Tsoi, Zh. Eksp. Teor. Fiz. 68, 1849 (1975) [Sov. Phys. JETP 41, 927 (1975)].

<sup>4</sup>A. M. Kosevich and I. M. Lifshitz, Zh. Eksp. Teor. Fiz. 29, 743 (1955) [Sov. Phys. JETP 2, 646 (1956)].

<sup>5</sup>I. M. Lifshitz and A. M. Kosevich, Zh. Eksp. Teor. Fiz. 33, 88 (1957) [Sov. Phys. JETP 6, 67 (1958)].

<sup>6</sup>Yu. P. Gaidukov and E. M. Golyamina, Pis'ma Zh. Eksp. Teor. Fiz. 23, 336 (1976) [JETP Lett. 23, 301 (1976)].

<sup>7</sup>Yu. P. Gaidukov, E. M. Golyamina, and N. P. Danilova, Prib. Tekh. Eksp. No. 2, 217 (1976).

<sup>8</sup>L. R. Windmiller and M. G. Priestley, Solid State Commun. 3, 199 (1965).

<sup>9</sup>N. B. Brandt, N. Ya. Minina, and Chu Chên Kang, Zh. Eksp. Teor. Fiz. 51, 108 (1966) [Sov. Phys. JETP 24, 73 (1967)].

<sup>10</sup>E. M. Golyamina and V. M. Pudalov, Prib. Tekh. Eksp. No. 6, 194 (1976).

<sup>11</sup>R. A. Herrod, C. A. Gage, and R. G. Goodrich, Phys. Rev. B 4, 1033 (1971).

<sup>12</sup>I. M. Lifshitz, M. Ya. Azbel', and M. I. Kaganov, Elektronnaya teoriya metallov, Nauka, M., 1971 (Electron Theory of Metals, Consultants Bureau, New York, 1973).

<sup>13</sup>D. Shoenberg, Phys. Kondens. Mater. 9, 1 (1969).

Translated by A. Tybulewicz